Continental Shelf Research 66 (2013) 49–57

Contents lists available at ScienceDirect

Continental Shelf Research

journal homepage: www.elsevier.com/locate/csr

Research papers

Temporal variation of summertime denitrification rates in the Texas–Louisiana inner shelf region in the Gulf of Mexico: A modeling approach using the extended OMP analysis

Il-Nam Kim *, Dong-Ha Min

Marine Science Institute, The University of Texas at Austin, Port Aransas, TX 78373, USA

ARTICLE INFO

Article history:
Received 14 February 2012
Received in revised form
9 July 2013
Accepted 15 July 2013
Available online 26 July 2013

Keywords:
Denitrification
Gulf of Mexico
Extended optimum multi-parameter analysis

ABSTRACT

The northern Gulf of Mexico (GOM) is well known for hypoxic water conditions ($O_2 \leq 2$ mg L^{-1}), and is often referred to as the "Dead Zone". The area of the Dead Zone has increased remarkably during the recent decades due to the increased coastal eutrophication. Under such conditions, denitrification process that removes "available nitrogen" from the system would likely become more active, and it needs to be better quantified to understand the nature of biogeochemical nitrogen cycles in the northern GOM. Despite its significance, few denitrification studies have been conducted for this area. We estimate the temporal variation of denitrification rates of the bottom waters at the northern Gulf of Mexico encompassing the "Dead Zone" during July of the 1985–2007 period (except for 1988–1990). We use historic hydrographic data and the extended Optimum Multi-Parameter analysis. Denitrification rates of the bottom waters in the region have gradually decreased from 1985 to 1997, and then increased to 2007. The water mass mixing composition of bottom waters on the Texas–Louisiana inner shelf has changed since ~1997. The Texas–Louisiana Coastal Water part has increased and that of the Subtropical Underwater has decreased. This change appears to have influenced the denitrification rates in the study area. We suggest that denitrification rates of bottom waters in the northern Gulf of Mexico are controlled not only by biogeochemical factors (i.e. organic matter supply and remineralization), but also by physical factor (i.e. stratification and relative contributions from different water masses).

1. Introduction

Denitrification is a dissimilatory process in which bacteria use nitrate as electron acceptor instead of oxygen under low oxygen conditions. Nitrate (NO_3^-) is typically reduced to nitrite (NO_2^-), and then to nitrous oxide and di-nitrogen (N_2O and N_2) in the process. In the ocean environment, denitrification is directly related to modern climate change through N_2O production, which is a greenhouse gas (Nevison and Holland, 1997; Nevison et al., 2003; Naqvi et al., 2010), and indirectly to glacial–interglacial climate change via regulation of the nitrogen availability in the ocean, which can enhance biological pump along with iron fertilization (McElroy, 1983; Altabet et al., 1995; Ganeshram et al., 1995, 2000, 2002; Falkowski, 1997).

The northern Gulf of Mexico (GOM) is known for frequent hypoxic water conditions in the sub-surface coastal waters with very low dissolved oxygen concentration ($O_2 \leq 2$ mg L^{-1} or 62.5 μmol L^{-1}) and often referred to as the "Dead Zone". Hypoxia frequently develops during the summertime by combination of high biological production and strong stratification in the coastal waters (Wiseman et al., 1997). The area of the Dead Zone has increased remarkably during the recent decades due to the increased coastal eutrophication (Rabalais et al., 2002). The recent "Deepwater Horizon" oil spill event occurred in the northern GOM has raised a concern for potential development of more extensive hypoxia in the region. Under such conditions, denitrification will play a more active role in biogeochemical cycles in the northern GOM and it needs to be better quantified. It may also be an important link to N_2O production in the northern GOM.

Only a few denitrification studies have been published for this area despite the importance of the process in biogeochemical cycling of nitrogen. Denitrification flux in the northern GOM was estimated from sediment samples at 21–44 μmol N m^{-2} h^{-1} by Gardner et al. (1993) from the mass balance between decrease of net organic nitrogen concentration and increase of inorganic nitrogen (NH_4^+, NO_3^-, and NO_2^-) concentrations in July 1990, estimated at 91–462 (149.31 ± 58.19–406.37 ± 55.30) μmol N m^{-2} h^{-1} from sediment samples in July 1999 by Childs et al. (2002, 2003) using the acetylene inhibition technique, and estimated at 45–149 μmol N m^{-2} h^{-1} from sediment samples in August 2003 by Delaune et al. (2005) using the acetylene inhibition technique. The error in estimates of Childs et al. (2002) is reported at Table 1 of Childs et al. (2003). The results of

* Corresponding author. Tel.: +1 36 749 6741; fax: +1 361 749 6777.
E-mail address: ilnamkim@utexas.edu (I.-N. Kim).

0278-4343/$ - see front matter © 2013 Elsevier Ltd. All rights reserved.
http://dx.doi.org/10.1016/j.csr.2013.07.005

Table 1
The summertime physicochemical characteristics of four mixing end-members defined in the northern Gulf of Mexico used for the extended OMP analysis.

Parameter	End-members			
	SUW (HS&LT)	TLCW (HS&HT)	ADW (LS)	MDW (LS)
T (°C)	18.61 ± 0.30	29.59 ± 0.37	31.14 ± 0.60	29.35 ± 1.13
S (psu)	36.65 ± 0.07	35.32 ± 0.21	0 ± 0	0 ± 0
DO (μmol L^{-1})	100.8 ± 20.6	150.9 ± 59.0	259.4 ± 40.4	248.6 ± 28.9
P (μmol L^{-1})	0.25 ± 0.07	0.64 ± 0.46	1.00 ± 0	3.56 ± 1.06
N (μmol L^{-1})	7.00 ± 1.56	3.23 ± 5.07	31.00 ± 0	126.51 ± 35.16
Si (μmol L^{-1})	11.10 ± 3.11	13.50 ± 6.91	90.70 ± 0	112.90 ± 40.56

H(L)S: high(low) salinity, H(L)T: high(low) temperature.
SUW: Subtropical Underwater, TLCW: Texas–Louisiana Coastal Water.
ADW: Atchafalaya Discharge Water, MDW: Mississippi Discharge Water.

Childs et al. (2003) are much higher than those of other two groups. Considering generally high level of variability of coastal oceans, it is difficult to determine whether these diverse estimates are at norm or anomalies, without the information on temporal variation and the type of techniques used to estimate denitrification.

To address these issues we conduct a study to: (1) estimate the denitrification rates in the inner continental shelf area of the northern GOM by using the long-term hydrographic data (1985–2007) and the extended Optimum Multi-Parameter (OMP) analysis, (2) model the temporal variation of denitrification rates, and (3) determine probable factors causing temporal variation in denitrification rates in the northern GOM.

2. Materials and methods

2.1. Data

The summertime Texas–Louisiana shelf-wide cruise data are obtained from http://www.nodc.noaa.gov (1985–1987, 1991–1993, and 1998–2007 periods) and http://www.aoml.noaa.gov/ocd/necop/ (1994–1997) sites. The selected study area is a broad continental shelf (bottom depth < 100 m) with two large river systems, the Mississippi and Atchafalaya Rivers (Fig. 1). The parameters used for the extended OMP analysis are latitude, longitude, depth, temperature (T), salinity (S), dissolved oxygen (DO), nitrate+nitrite (N), phosphate (P), and silicate (Si). Nutrient measurements were made at only two depths during the original hydrographic surveys: near surface (i.e. ca. 1 m from surface) and near bottom (i.e. ca. 1 m from the bottom). The surface and bottom T, S, and DO data are selected at the depths of nutrient measurements to use the data from the same depths in the extended OMP calculations.

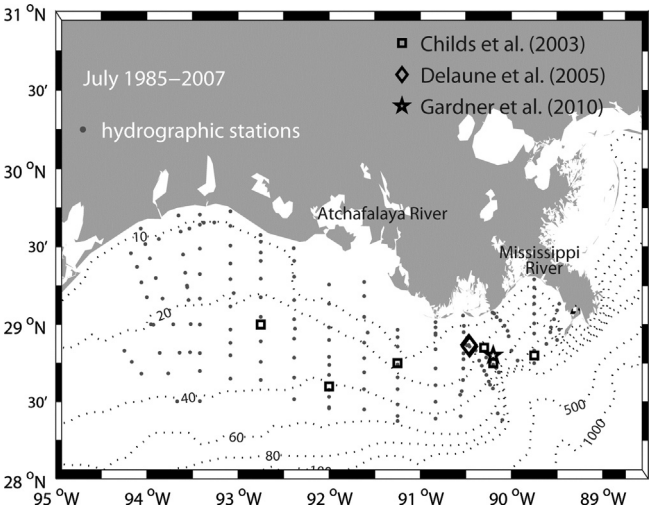

Fig. 1. The study area map. Texas–Louisiana shelf-wide cruises were conducted regularly by LUMCON (The Louisiana Universities Marine Consortium) since July 1985. All sampling station locations (dots) for the July 1988–1990, except for July 1988–1990, are shown with the sediment sampling sites of previous denitrification studies (square: Childs et al., 2003, diamond: Delaune et al., 2005, and star: Gardner et al., 2010) in the northern GOM. Note that we did not plot the sediment sampling locations of Gardner et al. (1993) as they did not provide the information of locations with number (Instead, see their Fig. 1).

2.2. The extended optimum multi-parameter (OMP) analysis

The magnitudes and changes of ocean properties are determined by physical mixing and biogeochemical processes (Anderson and Sarmiento, 1994). The extended OMP analysis is a useful way to quantify such conditions. The basic OMP analysis was originally developed to analyze physical mixing processes (Tomczak and Large, 1989). The Redfield ratios were later added in the calculations to analyze the influences of basic biogeochemical processes, and this version is called the "extended OMP analysis" (Karstensen and Tomczak, 1998). The extended OMP analysis was further improved to estimate the biogeochemical changes in remineralization, denitrification, and carbonate dissolution (Hupe and Karstensen, 2000). The extended OMP analysis is essentially an inverse method based on an over-determined linear system that has copious solutions for the unknown variables (i.e. number of equations is more than number of unknown variables). However, the solutions can be found by a non-negative least squares method (NNLS) (Tomczak and Large, 1989). The matrix structure of the extended OMP analysis used here is expressed as:

$$\underbrace{\begin{vmatrix} T_1 & + \cdots + & T_4 & + & 0 & + & 0 \\ S_1 & + \cdots + & S_4 & + & 0 & + & 0 \\ \mathrm{DO}_1 & + \cdots + & \mathrm{DO}_4 & - & r_{\mathrm{O}_2/P} & + & 0 \\ \mathrm{P}_1 & + \cdots + & \mathrm{P}_4 & + & 1 & + & r_\alpha \\ \mathrm{N}_1 & + \cdots + & \mathrm{N}_4 & + & r_{N/P} & - & 1 \\ \mathrm{Si}_1 & + \cdots + & \mathrm{Si}_4 & + & r_{\mathrm{Si}/P} & + & 0 \\ 1 & + \cdots + & 1 & + & 0 & + & 0 \end{vmatrix}}_{A} \times \underbrace{\begin{vmatrix} x_1 \\ x_2 \\ x_3 \\ x_4 \\ \Delta P_{remi} \\ \Delta N_{deni} \end{vmatrix}}_{x} - \underbrace{\begin{vmatrix} T_{obs} \\ S_{obs} \\ \mathrm{DO}_{obs} \\ \mathrm{P}_{obs} \\ \mathrm{N}_{obs} \\ \mathrm{Si}_{obs} \\ 1 \end{vmatrix}}_{d} = \underbrace{\begin{vmatrix} R_T \\ R_S \\ R_{\mathrm{DO}} \\ R_{\mathrm{P}} \\ R_{\mathrm{N}} \\ R_{\mathrm{Si}} \\ R_{\mathrm{MC}} \end{vmatrix}}_{R} \quad (1)$$

where, the matrix A is defined by the physicochemical characteristics of water masses, the Redfield ratios ($r_{\mathrm{O}_2/\mathrm{P}}$, $r_{\mathrm{N}/\mathrm{P}}$, and $r_{\mathrm{Si}/\mathrm{P}}$), and r_α (1/104) to estimate the amount of phosphate remineralized by denitrification (Gruber and Sarmiento, 1997; Hupe and Karstensen, 2000), the column x is composed of relative mixing ratios of x_i among water masses, the amount of remineralized phosphate ($\Delta \mathrm{P}_{remi}$), and the amount of denitrification ($\Delta \mathrm{N}_{deni}$), the next column d contains observation data for the physicochemical properties, and the last column R represents residuals from the extended OMP calculation for each parameter. The last row of the

matrix consisting of "1" constrains mass conservation among the source water masses ($\sum_{i=1}^{n} x_i = 1$). The computations of the extended OMP analysis are carried out by (1) defining the physicochemical characteristics of source water types (or end-member types) to form the matrix A, (2) assigning the Redfield ratios ($r_{N:P:Si:-O_2}$) to the matrix A, (3) estimating the weights of each parameter, and (4) finding the non-negative solutions for x_i, ΔP_{remi}, and ΔN_{deni} by minimizing the residual. An extended OMP program written in MATLAB™ was used in the analysis (http://www.ldeo.columbia.edu/~jkarsten/omp_std/)

The detailed information on physicochemical characteristics of end-members, assignment of Redfield ratios, weights for each parameter, validation for the extended OMP analysis, and limitations for the extended OMP analysis is described in below (Sections 2.2.1–2.2.5).

2.2.1. Physicochemical characteristics of end-members

We use temperature and salinity data collected in the Texas–Louisiana shelf region during the July 1985–2007 period, except for July 1988–1990, to investigate physical properties of waters on a T–S diagram (Fig. 2). Based on the data distribution pattern, three different end-members are assumed to participate in mixing process in the study area: low temperature and high salinity waters, high temperature and high salinity waters, and high temperature and low salinity waters. Geographical locations and temperature and salinity properties based on T–S diagram used to define the physicochemical characteristics of end-members are as follows (Fig. 3). Low temperature and high salinity waters are ranged from $18 \le T \le 19$ and $35.2 \le S \le 37.5$ on the T–S diagram. We adopt mean values of physicochemical properties of two stations that satisfy these conditions as characteristics of end-member 1 (Fig. 3a). The end-member 1 is at salinity maximum (Fig. 2). Salinity maximum waters are the Gulf Water (GW; $36.4 \le S \le 36.5$) in the western GOM and the Subtropical Underwater (SUW; $S > 36.5$) in the eastern GOM (Morrison et al., 1983; Vidal et al., 1994). The end-member 1 is geographically close to the GW, but the salinity characteristic ($S = 36.65$) is greater than that of GW. SUW enters the western GOM with the Loop Current (Jochens and DiMarco, 2008). The temperature and density of end-member 1 ($T = 18.61$ and $\sigma_t = 26.4$) appears similar to those of Eighteen Degree Water (EDW) from the Sargasso Sea, but EDW is distinct with its oxygen maximum (3.6–3.8 ml l^{-1} or 161–170 μmol L^{-1}) and lower salinity at about 36.3 (Morrison and Nowlin, 1977). The water properties of EDW, except for temperature, do not fit those of end-member 1. We thus define the end-member 1 as SUW. High temperature and high salinity waters ($29 \le T \le 30$ and $35 \le S \le 37$ on the T–S diagram), end-member 2, are distributed widely in the study area (Fig. 3b). The mixture of Mississippi and Atchafalaya discharge waters and inner shelf waters spreads as the Texas–Louisiana Coastal Current (TLCC) (Wiseman and Kelly, 1994; Jarosz and Murray, 2005). TLCC occupies large part of the study area, and flows seasonally along the Texas–Louisiana coast. Thus, we refer to the end-member 2 as the Texas–Louisiana Coastal Water (TLCW). Two large rivers contribute fresh surface waters in the study area; the Mississippi River (~70%), and the Atchafalaya River (~30%) (Dagg and Breed, 2003). We distinguish these two rivers by their geographic locations. The nutrient concentrations of the Mississippi River water are substantially higher than those of Atchafalaya River water (Pakulski et al., 2000).

The physicochemical characteristics of end-member 3, Atchafalaya Discharge water (ADW), are defined by $S \le 5$ and longitude: west of 91 W. Several stations near the plume of Atchafalaya River inshore of 20 m isobath belong to this group (Fig. 3c). Although the physical properties are similar among the selected stations, their chemical properties (N, P, and Si) are distinct. Temperature, salinity, and oxygen characteristics of ADW are defined by averaging data from the different stations (Fig. 3c). The characteristics of nitrate+nitrite (N), phosphate (P), and silicate (Si) of ADW are selected from a station at the plume of Atchafalaya River (square symbol in Fig. 3c), where N, P, and Si concentrations are highest among the stations. Two stations at the mouth of the Mississippi River mouth are selected for the end-member 4, the Mississippi Discharge Water (MDW), with $S \le 5$ and longitude: east of 90W conditions (Fig. 3d). Only the nutrient concentrations were originally measured at the mouth of Mississippi River during the Texas–Louisiana shelf-wide cruises with no physical property measurements (Table 3). Thus, the temperature, salinity, and oxygen characteristics of MDW are defined by averaging those two stations' data shown in Fig. 3d, and its chemical characteristics (N, P, and Si) are selected from the mean values shown in Table 2. Note that the salinity characteristics of ADW and MDW are assumed as zero at the river mouths. The defined characteristics of end-members used in the extended OMP analysis are summarized in Table 1.

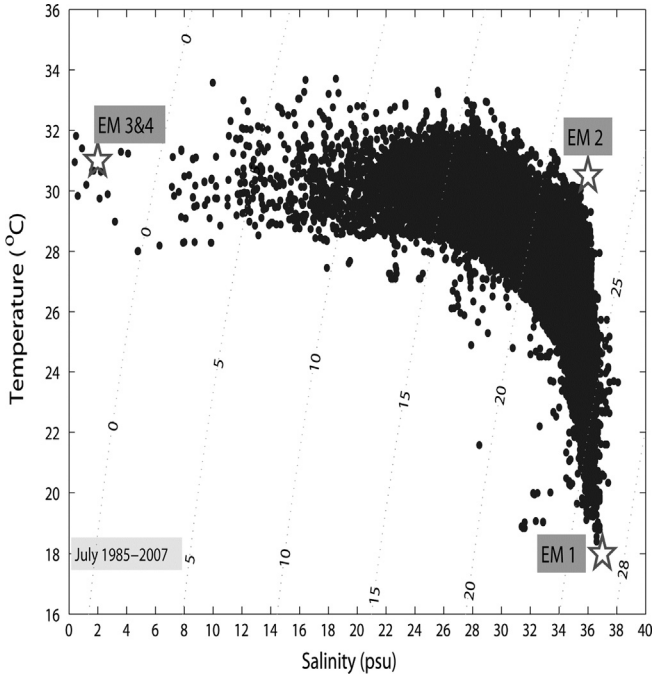

Fig. 2. A temperature-salinity diagram for the study area in GOM during the study period (July of 1985–2007; except for July 1988–1990). The end-members (stars) and distributions of their physical characteristics are shown in the diagram.

2.2.2. Assignment of Redfield ratios

The extended OMP analysis accounts for the effects of biogeochemical processes by using the Redfield ratios. In general, the Redfield ratios are estimated through linear regression analysis with the nutrient data. Our dataset shows, however, wide scatters of P and N, so appropriate numbers cannot be defined with the regression analysis. We consider, therefore, 4 different cases of different Redfield ratios: (1) the traditional Redfield ratios (Redfield et al., 1963), $r_{N:P:-O_2} = 16{:}1{:}138$, (2) slightly revised Redfield ratios, $r_{N:P:-O_2} = 16{:}1{:}150$ (Anderson, 1995), (3) a simple average N:P ratio of individual samples ($= [\sum_{i=1}^{n} N_i^{obs}/P_i^{obs}]/n$) in the study area, $r_{N:P:-O_2} = 11{:}1{:}138$, and (4) a simple average N:P ratio in the study area with slightly different $r_{P:-O_2}$, $r_{N:P:-O_2} = 11{:}1{:}150$. The silicates regenerated in the water column are the result of remineralization and dissolution (Park, 1967; Kido and Nishimura, 1973). The part of remineralization is represented by the ratio of Si/P, and the dissolution part is placed on the column vector x as an unknown variable.

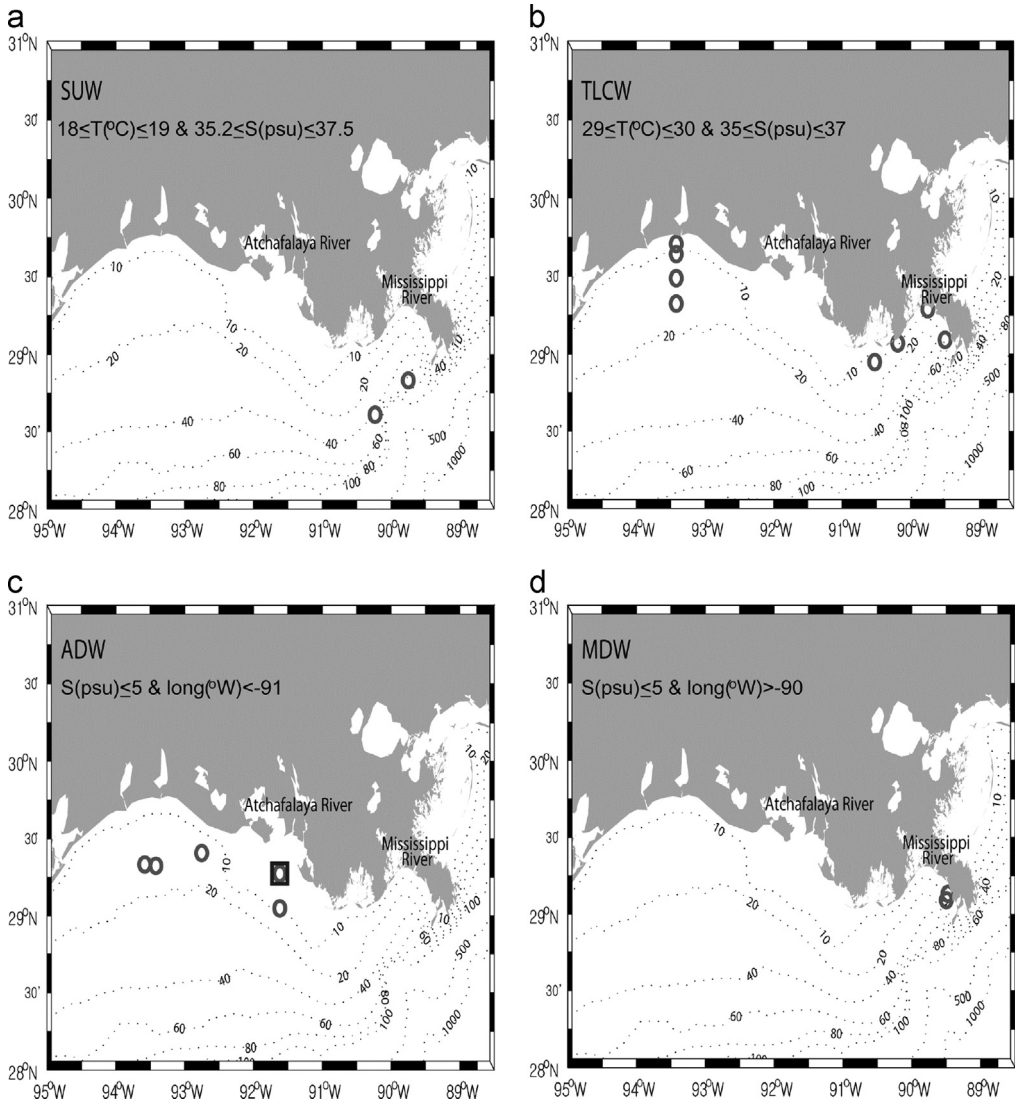

Fig. 3. Hydrographic stations (circles) used to determine physicochemical characteristics of 4 end-members. (a) Subtropical Underwater (SUW), (b) Texas–Louisiana Coastal Water (TLCW), (c) Atchafalaya Discharge Water (ADW), (d) Mississippi Discharge Water (MDW). The square station in (c) was selected to define the nutrient characteristics of ADW.

Table 2
The observed N and P concentrations at the mouth of the Mississippi River for July of 1993–2007 period.

Year	NO_2+NO_3 (μmol L^{-1})	PO_4 (μmol L^{-1})	Si (μmol L^{-1})
1993	150	5.50	167.7
1994	101.3	4.20	103.5
1995	95.2	2.90	117.3
1996	222.2	4.30	107.8
1998	150.5	3.40	128.6
1999	117	3.60	120.4
2000	136.3	3.40	127.0
2001	119.2	5.00	138.8
2002	157.1	1.00	62.7
2003	94.1	2.90	61.4
2004	113	3.50	168.3
2005	121	3.60	99.4
2006	95.6	3.00	27.5
2007	98.6	3.60	149.76
Mean ± std	126.5 ± 35.2	3.56 ± 1.06	112.9 ± 40.6

Table 3
Four cases of different Redfield ratios ($r_{N:P:Si:-O_2}$) used for the extended OMP analysis (see details in Section 2.2.2).

Parameter	Redfield ratios (N:P:Si:−O_2) Case			
	1	2	3	4
N	16	16	11	11
P	1	1	1	1
Si	15	15	16	16
O_2	138	150	138	150

The extended OMP analysis is based on over-determined system with more known equations (number of rows) than unknown variables (number of columns). So the addition of a new unknown variable to the column vector x makes it an even-determined system of equal number of equations and the unknown variables. In addition, the remineralization and dissolution processes are difficult to distinguish in the shallow coastal water environment. Thus, the ratio of Si/P is assumed to represent the mixed results of remineralization and dissolution. We use the Si/P ratio of 15 for the cases 1 and 2 (Redfield et al., 1963), and 16 for the cases 3 and 4, that were previously estimated in the northern GOM (Justic et al., 1995) (Table 3).

2.2.3. Weights for each parameter

The parameters for the extended OMP analysis contain different precisions and accuracies from each other. Appropriate weights can be assigned to each parameter to consider this matter (Tomczak and Large, 1989)

$$W_j = \frac{\sigma_j^2}{\delta_{j\max}} \tag{2}$$

where, $\sigma_j{}^2$ is the variance of parameter j calculated from the physicochemical characteristics of end-members defined, and $\delta_{j\max}$ is the largest among the variances of parameters estimated in the source regions for each end-member. Since we cannot have the information on $\delta_{j\max}$, we use a different weight equation previously applied to a marginal sea system (Kim and Lee, 2004). The weight equation is written as

$$W_j = \frac{\sigma_j}{\text{accuracy}_j} \tag{3}$$

where, σ_j is the standard deviation of parameter j calculated from the physicochemical characteristics of end-members defined. It allows each parameter j to distinguish end-members (Leffanue and Tomczak, 2004). The accuracy$_j$ is defined as the measurement error of parameter j. The weights used for the extended OMP analysis are summarized in Table S1.

2.2.4. Validation of the extended OMP analysis

The extended OMP analysis is based on over-determined system, which means that there can be multiple copious solutions, but it ultimately finds a best solution by minimizing the residuals. The residuals provide a way to evaluate determination of number of end-members and the validation of solutions (Tomczak and Large, 1989). The residuals of mass conservation (R_{MC}), for example, are calculated as follows:

$$R_{MC}(\%) = \left(\sum_{i=1}^{4} x_i - 1\right) \times 100 \tag{4}$$

The salinity distinguishes the end-members (ADW and MDW vs. TLCW vs. SUW) clearly in the study area. The plot of Salinity vs. R_{MC} is used to determine which waters have high residuals. The residuals increase slightly near the salinity of 36, which is a mixture of TLCW and SUW, but overall the residuals are well constrained within ~2% (Fig. 4). Poor choices of end-members or their characteristics would have resulted in larger residuals.

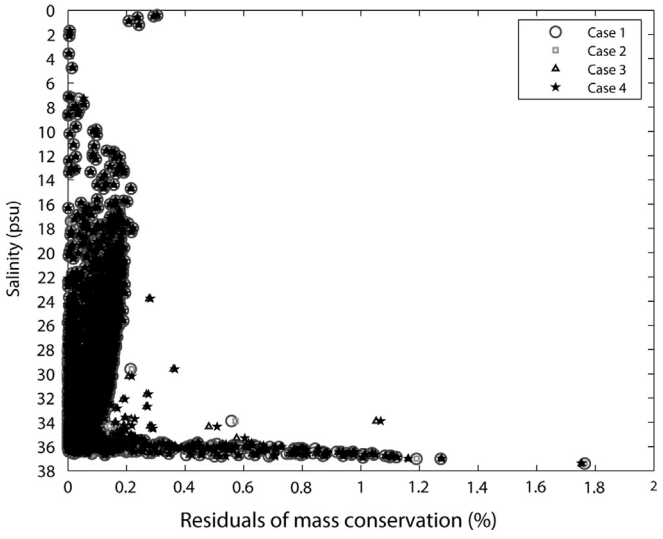

Fig. 4. The plot of salinity vs. residuals of mass conservation for 4 Redfield ratio cases. The pattern shows how the solutions follow the constraint of mass conservation, $\sum_{i=1}^{n} x_i = 1$. The residuals are slightly increasing near 36 psu of salinity, but overall they are well confined within ~2%.

2.2.5. Limitations for the extended OMP analysis

The extended OMP analysis can be used with any hydrographic data (Tomczak and Large, 1989), and it requires good definitions of physicochemical characteristics of end-members at their source regions. In general, however, it is difficult to define pure end-members in coastal oceans due to high spatiotemporal variability, lack of source water information, and insufficient long-term hydrographic data. We defined the 4 different end-members (i.e. ADW, MDW, TLCW, and SUW) and their physicochemical characteristics with the data obtained in the study area (Table 1). Although the currently defined characteristics of end-members (see Section 2.2.1) do not completely fulfill the needs to be defined at the actual source regions, since the observations were conducted in the same area of the northern GOM for the July season over 20-year of period (see details in Section 2.1), the characteristics defined with the long-term data can represent the system within particular space and time.

The end-member characteristics of ADW and MDW are defined near the mouth of Atchafalaya and Mississippi Rivers (Fig. 3c and d), of TLCW in the shallow inner shelf area, and of SUW south of the Mississippi River delta where a branch of SUW approaches onshore along with the Loop Current (LC) or Loop Current Eddies (LCEs). SUW enters GOM through the Yucatan Channel along with LC as a shallow salinity maximum (Jochens and DiMarco, 2008), after it is formed by subduction in subtropical Atlantic Ocean (O′Connor et al., 2005).

We assume that the currently defined end-member properties can represent the source water contributions for the study area although they may not be the actual source waters at the original formation areas. Therefore, SUW contribution in our analysis is indeed a contribution of the 'modified' SUW in the northern GOM, as we cannot account for the property changes between the formation area and the study area for SUW.

The end-member definitions are significantly important in the extended OMP analysis, because the solutions can be underestimated or overestimated if wrong information on them is used for the extended OMP analysis. Although we defined the end-member characteristics with the long-term hydrographic data and the residuals of mass conservation were within ~2% (Fig. 4), there might be still potential error in terms of the definitions of end-member characteristics.

Considering the limitations above, we confine that the end-member characteristics and the results (x_i, ΔP, and ΔN) from the extended OMP analysis are valid within the study area and July of summer season only. In addition, we assume that the effect of wintertime source water conditions is insignificant during the summertime since the study area is shallow (< 100 m) and does not show the bottom topography that may entrap significant waters with wintertime signatures (Fig. 1).

3. Results

3.1. Temporal variation of bottom water mixing ratios among end-members

The composition of the bottom waters (i.e. mixing ratios for individual end-members) in the study area exhibits a significant temporal variability over time (Fig. 5). The contributions from SUW and TLCW dominate the composition of the bottom water (> 90%), whereas the contributions from the River inflows (ADW and MDW) are insignificant in the bottom water (Fig. 5). Since the

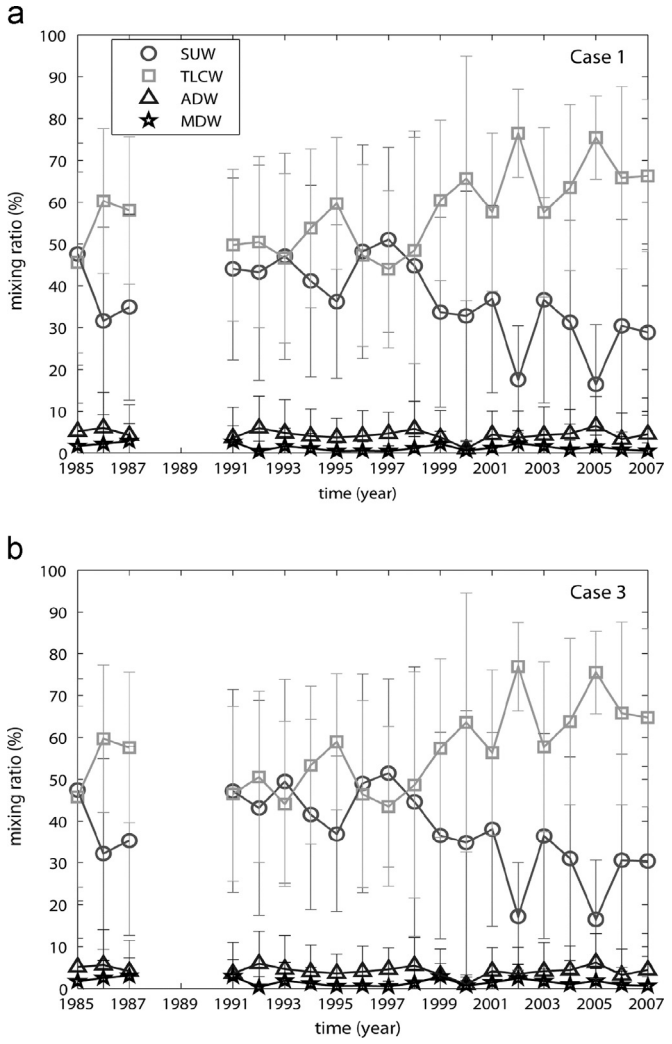

Fig. 5. The temporal variability of mean mixing ratios among the Subtropical Underwater (SUW), Texas–Louisiana Coastal Water (TLCW), Atchafalaya Discharge Water (ADW), and Mississippi Discharge Water (MDW) in the study area. (a) Mixing ratios with Case 1 ($r_{N:P:Si:\ -O_2}$=16:1:15:138), and (b) with Case 3 ($r_{N:P:Si:-O_2}$=11:1:16:138). Error bars represent standard deviation (Table S2).

4 Redfield ratios used in the analysis do not differ greatly, only results of cases 1 ($r_{N:P:Si:-O_2}$=16:1:15:138) and 3 ($r_{N:P:Si:-O_2}$=11:1:16:138) are shown in Fig. 5. The results of the cases 2 and 4 are shown in Table S2, along with the estimated mixing ratios with individual cases. The mixing ratios of SUW and TLCW show little variation with time until 1997. Since then, the SUW fraction for the bottom water has decreased gradually, whereas the TLCW fraction has increased with time, indicating that the bottom water composition in the study area can change substantially with time. TLCW has dominated the bottom water composition in the study area during the 2000s.

The water temperature characteristic helps distinguish SUW (colder) from TLCW (warmer) (Table 1). The mean temperatures of the surface and the bottom waters have increased significantly during the study period (Fig. 6). Since our datasets are mere snapshots obtained only in July time at a highly variable and dynamic coastal ocean environment, one cannot relate this phenomenon to climate change. However, the bottom waters have been occupied predominantly by warmer TLCW in the recent period is likely related to large-scale circulation processes in GOM. The potential effects of bottom water compositional changes to denitrification rates are explored below.

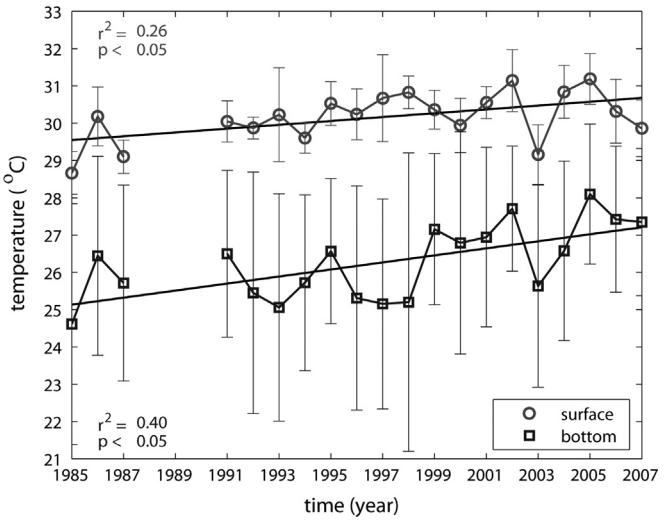

Fig. 6. The changes of surface and bottom temperatures in the study area of northern GOM between 1985 and 2007 (except for 1988–1990). Error bars represent standard deviation. *P* values were calculated by *t*-test (n=20).

3.2. Estimation of denitrification rates

Denitrification likely occurs in suboxic ($O_2 \leq 4.5\ \mu mol\ L^{-1}$ = 0.1 ml L^{-1} = 0.14 mg L^{-1}) condition (Naqvi et al., 2010). Significant denitrification ($\Delta N_{deni} > 0$) and suboxia are found only at the bottom waters in the study area. However, denitrification signals estimated from the extended OMP analysis derived from bottom waters cannot be distinguished from those derived from sediments. The thickness of the bottom layer (ΔH) is 1 m on average. Here, we assume that denitrification is occurring in a bottom layer that includes both bottom waters and sediments. All the water properties are assumed to be vertically uniform in this layer. The unit of denitrification estimated by the extended OMP analysis (Eq. (1)) is given as concentration, $\mu mol\ L^{-1}$ (or, $mmol\ m^{-3}$). Time and volume (m^3) data are necessary to transform the concentration unit to a rate. We estimate the denitrification rates only for the study area (mean area; $\overline{A}$); that is approximately $3.24 \times 10^{10}\ m^2$. We also assume that the denitrification rate is constant during July time period (ΔT). Since we have no information on significance of anaerobic ammonium oxidation (Anammox) and dissimilatory nitrate reduction to ammonium (DNRA) in nitrogen loss in the study area, we also assume that denitrification (ΔN_{deni}) alone is a major nitrogen sink in the study area. With the above assumptions, the denitrification rate can be expresses as:

$$\text{deni. rate}\left(\text{Gg N mon}^{-1}\right) = \overline{\Delta N}_{deni}\left(\frac{\text{mmol}}{\text{m}^3}\right) \times \frac{14\ \text{g N}}{1\ \text{mol}} \times \overline{A}(\text{m}^2) \times \Delta H(\text{m}) \times \Delta T(\text{mon})^{-1} \quad (5)$$

where, $\overline{\Delta N}_{deni}$ is the mean denitrification within the study area, and G denotes Giga or 10^{-9}. The estimated mean denitrification ($\overline{\Delta N}_{\text{deni}}$) or denitrified nitrogen concentration is $5.83 \pm 2.68\ mmol\ m^{-3}$, and the mean denitrification rate is $3.40 \pm 1.80\ Gg\ N\ mon^{-1}$.

3.3. Temporal variation of denitrification rates

The estimated denitrification rates show substantial variability with time in the study area (Fig. 7) at the ranges of 2.22 ± 3.06 to $13.50 \pm 9.98\ Gg\ N\ mon^{-1}$ and 1.05 ± 3.06 to $4.73 \pm 4.15\ Gg\ N\ mon^{-1}$ for the Redfield ratio cases of 1 and 3, respectively (Table S3). The denitrification rates had gradually decreased from 1985 to 1997. Since July 1997, when the denitrification rate was lowest, the

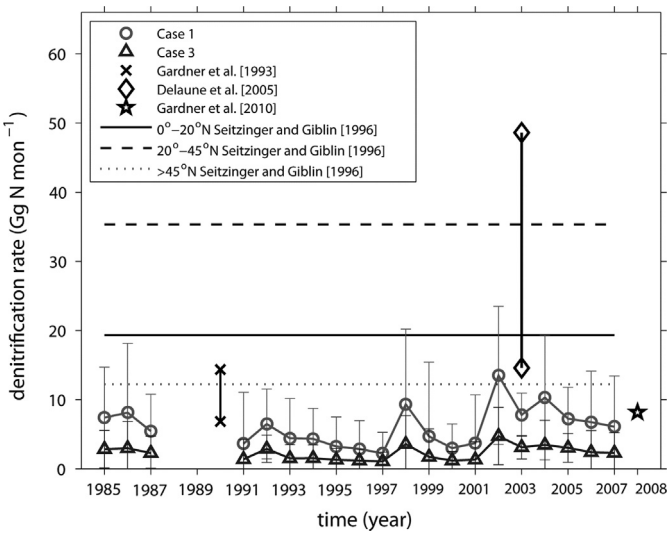

Fig. 7. The temporal variability of mean denitrification rates (Gg N mon^{-1}) in the study area. Different symbols indicate the denitrification rates with Case 1 (circle), the denitrification rates with Case 3 (triangle), and three other previous estimates in the study area (cross for Gardner et al., 1993, diamond for Delaune et al. (2005), and star for Gardner et al., 2010). Different line styles represent the latitudinal mean denitrification rates at 0–20°N (solid line), 20–45°N (broken solid line), and >45°N (dotted line), respectively, in the North Atlantic continental shelf regions (Seitzinger and Giblin, 1996). Error bars represent standard deviation (Table S2). Note that the result of Childs et al. (2003) was not included in this Fig. for better resolution as its range (~30–151 Gg N mon^{-1}) was not comparable with other estimates.

denitrification rates have increased with time to 2007, with somewhat large variation.

Three other previous estimates obtained in the similar area (Gardner et al., 1993; Childs et al., 2003; Delaune et al., 2005) and the latitudinal mean denitrification rates (at 0–20°N, 20–45°N, and >45°N) in the North Atlantic continental shelf regions (Seitzinger and Giblin, 1996; See their Table 1) are compared to the current estimates (Fig. 7). A denitrification rate recently measured from the sediments in July 2008 at the same study area by Gardner et al. (2010; unpublished data, ~25 μmol N m^{-2} h^{-1} at 28.8°N/90.2°W) using the Membrane Inlet Mass Spectrometer (MIMS) system is fairly consistent with the current estimates (Fig. 7), even though just one station is available. The literature values are converted to the unit of Gg N mon^{-1} by multiplying $\overline{A}\approx 3.24\times10^{10}$ m^2 for the study area. Overall, the estimated denitrification rates of the current study are similar to the mean denitrification rates of the latitudinal bands of 0–20°N and >45°N in the North Atlantic Ocean (Fig. 7). The previous estimates, made in July 1990 (6.85–14.36 Gg N mon^{-1}) by Gardner et al. (1993), in August 2003 (14.6–48.6 Gg N mon^{-1}) by Delaune et al. (2005), and in July 2008 (~8.17 Gg N mon^{-1}) by Gardner et al. (2010) are comparable to the current analysis within the given standard deviations, even though the upper bound value of Delaune et al. (2005) is somewhat higher (Fig. 7). Although the lower bound value (~30 Gg N mon^{-1}) of Childs et al. (2003) resembles the estimates of this study, their upper bound value (~151 Gg N mon^{-1}) is much higher than the current estimates and the latitudinal mean denitrification rates of the North Atlantic continental shelf regions (Fig. 7). Childs et al. (2002) described sediment denitrification in the northern GOM, and their estimates were comparable to the estimated values (Gardner et al., 1993, 2010; Delaune et al., 2005) and the modeled values from this study. However, later Childs et al. (2003) reported the erratum on their estimation of denitrification rates due to the use of wrong gas constant. They did not provide additional description with the corrected denitrification rates. Furthermore, their upper bound value (~150 Gg N mon^{-1}) is much higher than all other literature values, so we suppose that their high values may be an overestimate. Direct denitrification measurements within short time intervals are necessary to accurately estimate the representative values for this region of high spatiotemporal variation. The details of the estimated denitrification rates are summarized in Table S3.

4. Discussions

4.1. The effect of water mass distributions on denitrification rate

Potential factors causing the low denitrification rate in July 1997 and high rate in July 2002 (Fig. 7) are considered. The distributions of water mass mixing ratios (as mean values of the cases 1–4) of SUW and TLCW for the bottom water are shown in Fig. S1, along with a contour line of DO=2 mg L^{-1} (or=65 μmol L^{-1}) as a demarcation of hypoxia in the area. A hypoxic condition developed widely in the study area in both years during July. On the other hand, the distributions of mixing ratios of SUW and TLCW were significantly different; SUW extended farther into the coast from offshore and TLCW was confined inshore within ~20 m isobath in July 1997 (Fig. S1a and c), whereas the SUW′s contribution was very weak and the TLCW′s occupation was widespread in July 2002 (Fig. S1b and d).

The meso-scale sea surface height anomalies (http://argo.colorado.edu/~realtime/gsfc_gom-real-time_ssh/) show that an anticyclonic (clockwise circulation) warm core eddy (89–92°W and 27–28.5°N) approached the southern boundary of the study area with an enhanced contribution of SUW in July 1997 (Fig. S1a and e); although warm eddies were separated from the LC near the study area in July 2002, they were not as close to the study area as in July 1997 with lesser input of SUW (Fig. S1b and f). SUW, originates in the subtropical Atlantic Ocean, enters GOM through the Caribbean Sea following LC. It spreads further into the interior of GOM along with LCEs that are separated from the main LC. The influence of SUW to the study area would likely depend on the extension of LC and the distribution of LCEs.

Denitrification rate depends generally on the availability of nitrate recycled through remineralization process, so it may correlate with the supply of organic matter in the water column. The enhanced presence of colder and saltier SUW in July 1997 presumably generated a stronger stratification of the water column with a steep vertical density gradient, and this pattern can reduce the supply of organic matter to the bottom layer in the study area. In addition, oligotrophic SUW contains lower nutrient concentrations. The bottom water N concentration (NO_3^-+NO_2^-) was much higher in July 2002 than that in July 1997 (Fig. S2). Therefore, the magnitude of extension of SUW may significantly influence the denitrification rate of bottom waters in the study area.

4.2. Correlations of denitrification rate with remineralization vs. water mass composition

Relationships among the denitrification rate, the amount of remineralized organic carbon, and the water mass mixing ratios are analyzed to examine the relationships between biogeochemical and physical factors. The amounts of denitrification (ΔN_{deni}) and remineralized phosphate (ΔP_{remi}), averaged from the cases 1–4 (Tables S3–4), are estimated by the extended OMP method. The amount of remineralized organic carbon for the rate of organic matter supply into the bottom layer is estimated from $\Delta P_{remi}\times 106$ ($r_{C:P}$) assuming that the amount of remineralized phosphate is positively correlated with the supply rate of organic matter following the Redfield ratios. The denitrification rate and the amount of remineralized carbon show a significant positive correlation (R=0.71) (Fig. 8a). The correlations between the denitrification rate

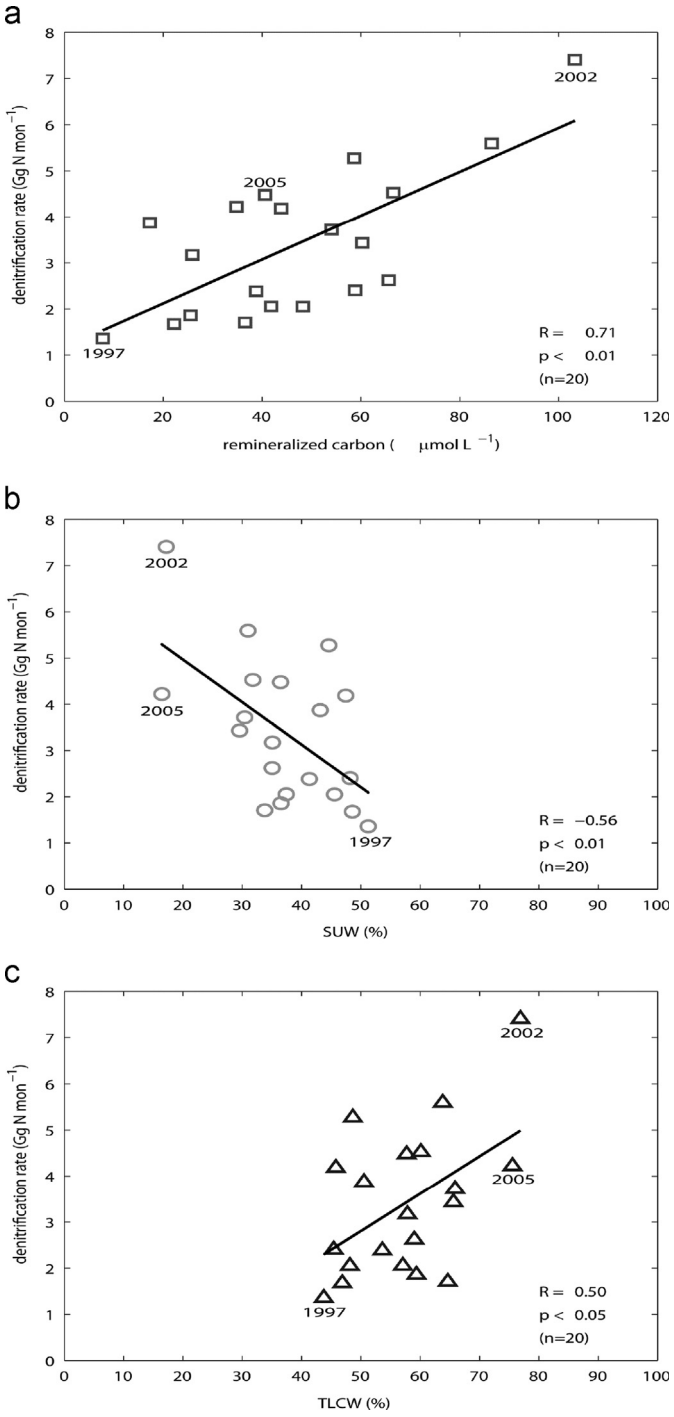

Fig. 8. Relationships between denitrification rate (Gg N mon^{-1}) and (a) the amount of remineralized carbon (μmol L^{-1}), (b) mixing ratios of SUW (%), and (c) mixing ratios of TLCW (%), with corresponding correlation coefficients (R). The mean values are averaged from the cases 1–4 (Tables S2–4). P values were calculated by t-test (n=20).

and SUW (Fig. 8b), vs. TLCW (Fig. 8c) are significantly negative ($R=-0.57$) and positive ($R=0.51$), respectively. The mean mixing ratio of SUW in the study area was higher in July 1997 than in July 2002 (Fig. 8b and Table S2), while the amount of remineralized carbon was much lower in July 1997 (≈8 μmol L^{-1}) than that in July 2002 (≈103 μmol L^{-1}) (Fig. 8a and Table S4).

The mean mixing ratio of SUW was lower again in July 2005 like in July 2002 (Fig. 8b and Table S2), but the denitrification rate ($=4.22\pm2.04$ Gg N mon^{-1}) in July 2005 was not similar to that in July 2002 ($=7.40\pm4.17$ Gg N mon^{-1}) (Fig. 8b and Table S3). It is due to the fact that the amount of remineralized carbon was lower in July 2005 (≈35 μmol L^{-1}) than that in July 2002 (≈103 μmol L^{-1}) (Fig. 8a and Table S4). We speculate that the supply of organic matters into the bottom layer was relatively higher in July 2002 than in July 2005.

In summary, the denitrification rates were low in July 1997, because SUW was dominant in the bottom waters with low remineralized carbon. The enhanced vertical density gradient might have impeded an input of organic matter into the bottom layer (i.e. negative connection between the biogeochemical factor: lower remineralization and the physical factor: enhanced stratification). On the other hand, the extent of SUW was limited and the amount of remineralized carbon was high in July 2002. The increased remineralization and reduced stratification might have caused higher denitrification rates (i.e. positive connection between the biogeochemical factor: increased remineralization and the physical factor: weakened stratification). Our analysis therefore indicates that the magnitude of denitrification rate does not necessarily correlate with the size of hypoxia in the study area. In the bottom layer of northern GOM, hypoxia can develop broadly in the study area by physical (stratification) and/or biogeochemical (remineralization) factors, but denitrification is determined by a rather competitive relationship between physical (stratification) and biogeochemical (remineralization) factors.

5. Conclusions

We present the magnitude and temporal variation of denitrification rates at the hypoxic area of the northern GOM during July 1985–2007 (except for July 1988–1990), estimated by the extended OMP analysis. The denitrification rates estimated at the bottom waters range from 1.36 ± 0.58 to 7.40 ± 4.17 Gg N mon^{-1} (for July and for the mean study area of 3.24×10^{10} m^2). The denitrification rates have gradually decreased from 1985 to 1997, and increased during the 1998–2007 period. The composition of bottom waters on the Texas–Louisiana inner shelf has changed since ~1997, with the increase of TLCW and decrease of SUW. This change appears to have influenced the denitrification rates at the bottom water layer in the study area. We found that the bottom water denitrification rates in the coastal northern Gulf of Mexico are controlled not only by organic matter supply (biogeochemical factor: remineralization), but also by the relative contribution from different water masses (physical factor: stratification).

Acknowledgments

We sincerely thank all the people who contributed to the Texas–Louisiana shelf-wide cruises for providing field data. We also thank Dr. Wayne S. Gardner (The University of Texas at Austin) for reading our manuscript and suggesting valuable comments. We also thank Dr. Nancy N. Rabalais (Louisiana Universities Marine Consortium) for providing the information on the access of Texas–Louisiana shelf-wide cruise data.

Appendix A. Supporting information

Supplementary data associated with this article can be found in the online version at http://dx.doi.org/10.1016/j.csr.2013.07.005.

References

Altabet, M.A., Francols, R., Murray, D.W., Prell, W.L., 1995. Climate-related variations in denitrification in the Arabian Sea from sediment 15 N/14 N ratios. Nature 373, 506–508.

Anderson, L.A., 1995. On the hydrogen and oxygen content of marine phytoplankton. Deep Sea Research Part I: Oceanographic Research Papers 42, 1675–1680.
Anderson, L.A., Sarmiento, J.L., 1994. Redfield ratios of remineralization determined by nutrient data analysis. Global Biogeochemical Cycles 8 (1), 65–80.
Childs, C.R., Rabalais, N.N., Turner, R.E., Proctor, L.M., 2002. Sediment denitrification in the Gulf of Mexico zone of hypoxia. Marine Ecology Progress Series 240, 285–290.
Childs, C.R., Rabalais, N.N., Turner, R.E., Proctor, L.M., 2003. Sediment denitrification in the Gulf of Mexico zone of hypoxia (Erratum). Marine Ecology Progress Series 274, 310.
Dagg, M.J., Breed, G.A., 2003. Biological effects of Mississippi River nitrogen on the northern Gulf of Mexico-a review and synthesis. Journal of Marine Systems 43, 133–152.
Delaune, R.D., Jugsujinda, A., Devai, I., Hou, A.X., 2005. Denitrification in bottom sediment near oil production facilities off the Louisiana Gulf Coast. Chemistry and Ecology 21 (2), 101–108.
Falkowski, P.G., 1997. Evolution of the nitrogen cycle and its influence on the biological sequestration of CO_2 in the ocean. Nature 387, 272–275.
Ganeshram, R.S., Pedersen, T.F., Calvert, S.E., Francois, R., 2002. Reduced nitrogen fixation in the glacial ocean inferred from changes in marine nitrogen and phosphorus inventories. Nature 415, 156–159.
Ganeshram, R.S., Pedersen, T.F., Calvert, S.E., McNeill, G.W., Fontugne, M.R., 2000. Glacial–interglacial variability in denitrification in the world's oceans: causes and consequences. Paleoceanography 15 (4), 361–376.
Ganeshram, R.S., Pedersen, T.F., Calvert, S.E., Murray, J.W., 1995. Large changes in oceanic nutrient inventories from glacier to interglacier periods. Nature 376, 755–758.
Gardner, W.S., Briones, E.E., Kaegi, E.C., 1993. Ammonium excretion by benthic invertebrates and sediment-water nitrogen flux in the Gulf of Mexico near the Mississippi River outflow. Estuaries 16 (4), 799–808.
Gardner, W.S., McCarthy, M.J., Xiao L., 2010. Denitrification as a Mechanism Causing Nitrogen Limitation of Microbial Activities at the Sediment Water Interface in the Hypoxic Region of the Eutrophic Northern Gulf of Mexico. 2010 Gulf Estuarine Research Society (GERS) Meeting, Port Aransas, TX.
Gruber, N., Sarmiento, J.L., 1997. Global patterns of marine nitrogen fixation and denitrification. Global Biogeochemical Cycles 11 (2), 235–266.
Hupe, A., Karstensen, J., 2000. Redfield stoichiometry in Arabian Sea subsurface waters. Global Biogeochemical Cycles 14 (1), 357–372.
Jarosz, E., Murray, S.P., 2005. Velocity and transport characteristics of the Louisiana–Texas coastal current: circulation in the Gulf of Mexico: observations and models. In: Sturges, W., Lugo-Fernandez, A. (Eds.), Geophysical Monograph Series 161, pp. 143–156.
Jochens, A.E., DiMarco, S.F., 2008. Physical oceanographic conditions in the deepwater Gulf of Mexico in summer 2000–2002. Deep Sea Research Part II: Topical Studies in Oceanography 55, 2541–2554.
Justic, D., Rabalais, N.N., Turner, R.E., 1995. Stoichiometric nutrient balance and origin of coastal eutrophication. Marine Pollution Bulletin 30 (1), 41–46.
Karstensen, J., Tomczak, M., 1998. Age determination of mixed water masses using CFC and oxygen data. Journal of Geophysical Research 103, 18599–18609.
Kido, K., Nishimura, M., 1973. Regeneration of silicate in the ocean. Journal of the Oceanographical Society of Japan 29, 185–192.
Kim, I.-N., Lee, T., 2004. Summer hydrographic features of the East Sea analyzed by the Optimum Multiparameter method. Ocean and Polar Research 26 (4), 581–594.
Leffanue, H., Tomczak, M., 2004. Using OMP analysis to observe temporal variability in water mass distribution. Journal of Marine Systems 48, 3–14.
McElroy, M.B., 1983. Marine biological controls on atmospheric CO_2 and climate. Nature 302, 328–329.
Morrison, J.M., Merrell, W.J., Key, R.M., Key, T.C., 1983. Property distributions and deep chemical measurements within the Western Gulf of Mexico. Journal of Geophysical Research 88, 2601–2608.
Morrison, J.M., Nowlin Jr., W.D., 1977. Repeated nutrient oxygen and density sections through the Loop Current. Journal of Marine Research 35, 105–128.
Naqvi, S.W.A., Bange, H.W., Farias, L., Monteiro, P.M.S., Scranton, M.I., Zhang, J., 2010. Marine hypoxia/anoxia as a source of CH_4 and N_2O. Biogeosciences 7, 2159–2190.
Nevison, C., Butler, J.H., Elkins, J.W., 2003. Global distribution of N_2O and the ΔN_2O–AOU yield in the subsurface ocean. Global Biogeochemical Cycles 17 (4), 1119, http://dx.doi.org/10.1029/2003GB002068.
Nevison, C., Holland, E., 1997. A reexamination of the impact of anthropogenically fixed nitrogen on atmospheric N_2O and the stratospheric O_3 layer. Journal of Geophysical Research 102, 25519–25536.
O'Connor, B.M., Fine, R.A., Olson, D.B., 2005. A global comparison of subtropical underwater formation rates. Deep Sea Research Part I: Oceanographic Research Papers 52, 1569–1590.
Pakulski, J.D., Benner, R., Whitledge, T., Amon, R., Eadie, B., Cifuentes, L., Ammerman, J., Stockwell, D., 2000. Microbial metabolism and nutrient cycling in the Mississippi and Atchafalaya River plumes. Estuarine, Coastal and Shelf Science 50, 173–184.
Park, K., 1967. Nutrient regeneration and preformed nutrients off Oregon. Limnology and Oceanography 12, 353–357.
Rabalais, N.N., Turner, E., Scavia, D., 2002. Beyond science into policy: Gulf of Mexico hypoxia and the Mississippi River. BioScience 52 (2), 129–142.
Redfield, A.C., Ketchum, B.H., Richards, F.A., 1963. The influence of organism on the composition of sea water: the sea: the composition of sea-water comparative and descriptive oceanography. In: Hill, M. N (Ed.), 2, pp. 26–77.
Seitzinger, S.P., Giblin, A.E., 1996. Estimating denitrification in North Atlantic continental shelf sediments. Biogeochemistry 35, 235–260.
Tomczak, M., Large, D.G.B., 1989. Optimum Multiparameter analysis of mixing in the thermocline of the Eastern Indian Ocean. Journal of Geophysical Research 94, 16141–16149.
Vidal, V.M.V., Vidal, F.V., Hernandez, A.F., Meza, E., Zambrano, L., 1994. Winter water mass distributions in the Western Gulf of Mexico affected by a colliding anticyclonic ring. Journal of Oceanography 50, 559–588.
Wiseman Jr., W.J., Kelly, F.J., 1994. Salinity variability within the Louisiana coastal current during the 1982 flood season. Estuaries 17, 732–739.
Wiseman, Wm.J., Rabalais, N.N., Turner, R.E., Dinnel, S.P., MacNaughton, A., 1997. Seasonal and interannual variability within the Louisiana coastal current: stratification and hypoxia. Journal of Marine Systems 12, 237–248.